Available online at www.sciencedirect.com
ScienceDirect
Thermochimica Acta 463 (2007) 2–5
thermochimica acta
www.elsevier.com/locate/tca

Short communication

Low temperature molar heat capacities and thermal stability of crystalline artemisinin

Jia-Xin Dong [a], You-Meng Dan [b], Zhi-Cheng Tan [c], Jun-Ning Zhao [c], Yi Liu [a,*]

[a] *College of Chemistry and Molecular Sciences, Wuhan University, Wuhan 430072, PR China*
[b] *Department of Chemistry, Hubei College of Nationality, Enshi 445000, PR China*
[c] *Thermochemistry Laboratory, Dalian Institute of Chemical Physics, Chinese Academy of Sciences, Dalian 116023, PR China*

Available online 7 April 2007

Abstract

The heat capacities of artemisinin in crystal form were measured in the temperature range from 80 to 363 K by an adiabatic calorimeter. Three thermal anomalies were observed at 198, 240, and 312 K. Thermogravimetry and differential thermal analysis from 300 to 700 K showed melting at 420 K, loss of formic acid at 480 K, and further decomposition above 480 K.

Keywords: Artemisinin; Heat capacity; Thermal stability

1. Introduction

Artemisinin (molecular structure: Fig. 1; formula: $C_{15}H_{22}O_5$; CAS RN: 63968-64-9; molecular mass: 282.33 g mol^{-1}) is a sesquiterpene lactone with an endoperoxide function. It was first isolated from the Chinese traditional herb—*Artemisia annua* L. and its structure was first confirmed by Chinese scientists in 1970s [1–6]. Artemisinin and its derivatives or analogues are currently regarded as the most promising weapons against multidrug-resistant malaria [7]. Its unique 1,2,4-trioxane structure is entirely incompatible with the traditional antimalarial structure–activity theory, which attracted the interesting of many researchers [7–10].

Chinese scientists working on artemisinin [5] and Lisgarten et al. [6] confirmed the crystal structure and the absolute configuration of artemisinin by X-ray diffraction. Lin et al. [11] and Luo et al. [12] studied the thermal rearrangement and decomposition products of it. Chan et al. [13] researched the polymorphism of artemisinin. Xing et al. [14] and Coimbra et al. [15] studied the solubility of artemisinin in supercritical carbon dioxide.

In the present work the heat capacities of artemisinin in crystal form were measured in the temperature range from 80 to 363 K by an adiabatic calorimeter. The thermal stability of the compound was further examined by thermogravimetry (TG) and differential thermal analysis (DTA) over the temperature range from 300 to 700 K.

2. Experimental

2.1. Materials

Artemisinin was obtained from Qingjiang Bioengineering Co. Ltd. (Ensi, Hubei, PR China). It was extracted from *Artemisia annua* L., and then purified. It is a colorless needle crystal and the purity of mass fraction was above 0.995, which was determined by HPLC and XRD. Further purification was not performed. Nitrogen gas with a purity of 99.999% was used in the TG–DTA test.

2.2. Adiabatic calorimetry

The heat capacity measurement was carried out in a small sample adiabatic calorimeter over the temperature range from 80 to 363 K. The detailed description of the adiabatic calorimeter was published in Refs. [16–19]. To verify the reliability of the adiabatic calorimeter, the molar heat capacity of synthetic sapphire (α-Al_2O_3, Standard Reference Material 720, NIST) was measured over the same temperature range. The mass of the α-Al_2O_3 used for the measurement was 8.7353 g. The deviations of the experimental results from the recommended values of NIST [20]

* Corresponding author. Tel.: +86 27 87218284; fax: +86 27 68754067.
E-mail address: prof.liuyi@263.net (Y. Liu).

0040-6031/$ – see front matter © 2007 Elsevier B.V. All rights reserved.
doi:10.1016/j.tca.2007.04.007

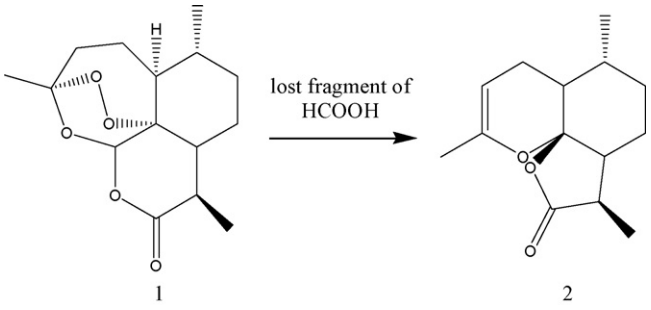

Fig. 1. The structure and thermal decomposition of artemisinin [11].

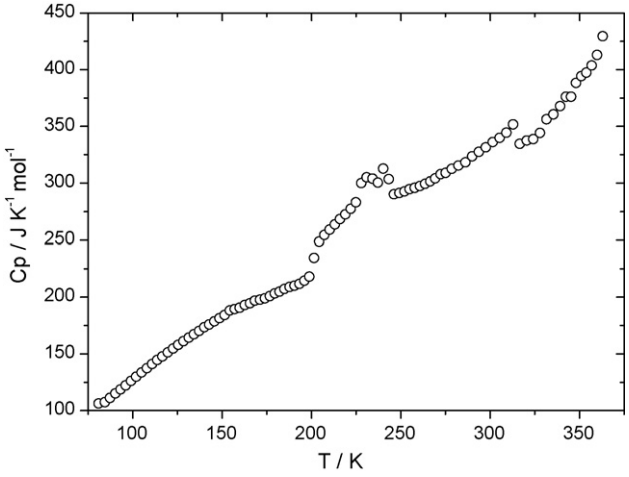

Fig. 2. Experimental molar heat capacities of artemisinin determined by adiabatic calorimetry.

were within ±0.5% over the entire temperature range of 80–387 K.

The mass of crystalline artemisinin used for the heat-capacity measurement was 2.9528 g, 10.4587 mmol, based on its molar mass of 282.33 g mol^{-1}. The sample was sealed in the calorimeter vessel and cooled down to 78 K by liquid nitrogen. Then the heat capacity measurement was initiated using the standard discrete heating method [16]. The duration of energy input was 10 min, and the thermal equilibrium inside the sample cell was attained within 3–5 min after the energy input. The temperature increment for each experimental point was about 3 K.

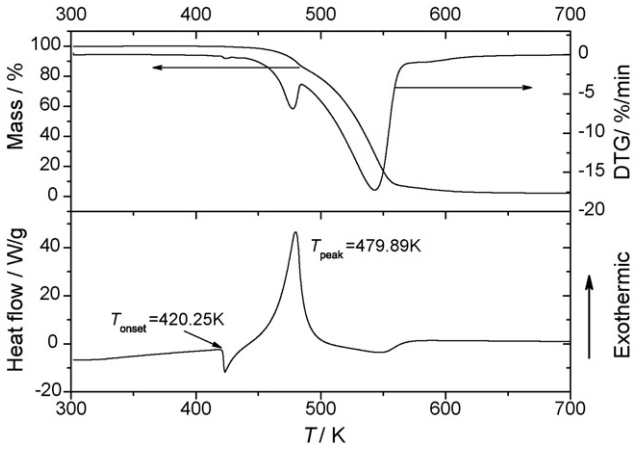

Fig. 4. TG–DTG–DTA curves of crystalline artemisinin.

2.3. The TG–IR analysis

TG–DTA–IR was performed in a thermal analyzer, SDT Q600 from TA instrument, USA. The instrument was calibrated with indium before the experiment. A sample mass of approximately 8 mg was used. The heating rate was 10 K min^{-1}, and the temperature range was from 300 to 700 K. The nitrogen gas flow rate was 200 mL min^{-1} to ensure that the gaseous decomposition products were quickly driven out from the furnace into the

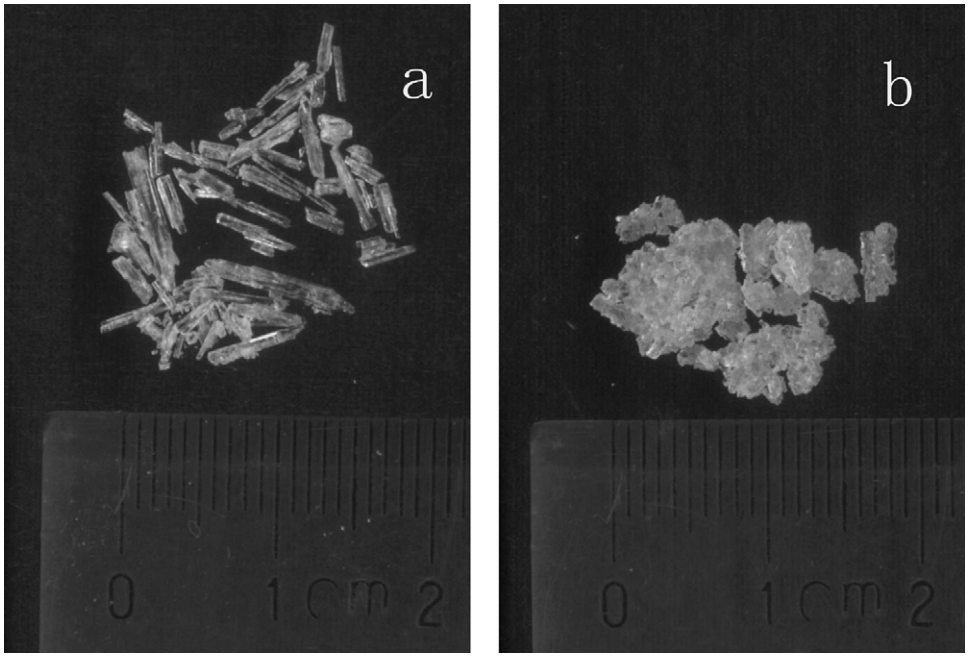

Fig. 3. The photographs of artemisinin crystal: (a) before and (b) after the adiabatic calorimetry.

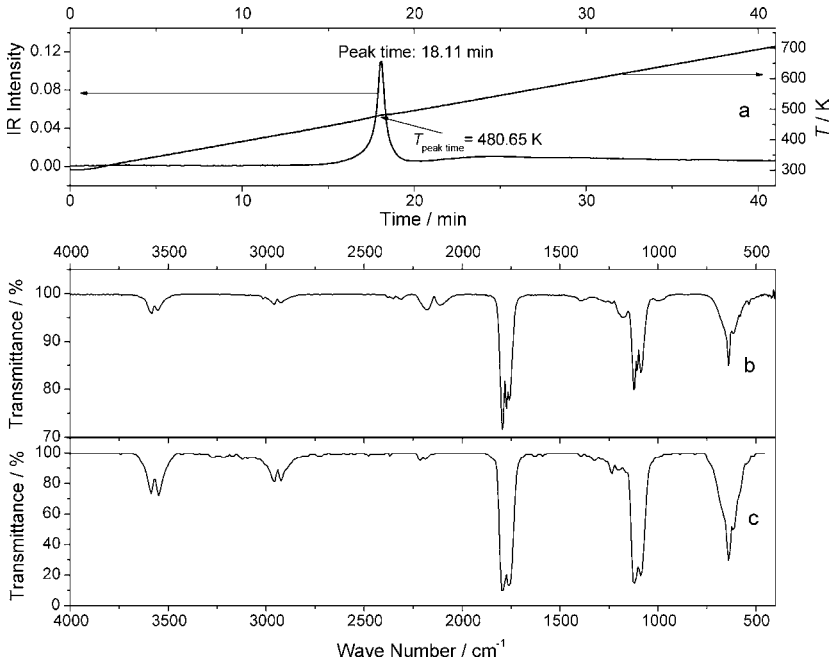

Fig. 5. The IR spectrum of the gaseous thermal decomposition products of artemisinin: (a) the IR absorbance intensity and sample temperature against time; (b) the IR spectrum of the carrier gas at peak time; (c) the standard IR spectrum of formic acid.

IR sample cell of Nicolet 380 with a TGA/FT-IR interface from Thermo Electron Corporation, USA. The temperature of the gas transfer tube and the sample cell of the IR were thermostated at 453 K. The IR background was collect and subtracted during the measurement.

3. Results

3.1. Heat capacity

Low-temperature heat capacities of artemisinin are shown in Fig. 2 and the supplementary data file. Three heat capacity abrupt changes were observed. The first one is at about 198 K. The heat capacities increased abruptly at this point, and then decreased abruptly at about 240 K. The third change takes place at about 312 K. The sample before calorimetric measurement was colorless needle crystal, however, after calorimetric measurement it transformed into granulose crystal, as shown in Fig. 3.

3.2. Thermal stability

The TG–DTG–DTA results are presented in Fig. 4. Most of the activities occur in the temperature range from 420 to 620 K in two steps. No residue was found in the crucible after the experiment. Two obvious peaks were observed in the DTA curve (heat flow). The first endothermic peak was associated with the fusion of artemisinin, at T_{onset} = 420 K. The second large exothermic peak corresponded to thermal rearrangement and decomposition, which starts just after the fusion and the peak temperature is 480 K.

The IR spectrum of gas is shown in Fig. 5. The peak of the IR absorbency intensity appeared just at the first mass loss step by comparing Figs. 4 and 5. By comparing the IR spectrum of the gas at the peak time with the standard IR spectrum library, as shown in Fig. 5, the gaseous decomposition products are mainly composed of formic acid (HCOOH) at this step. If artemisinin decomposed into the compound 2 as demonstrated in Fig. 1 according to Refs. [11,12], the lost fragment is just the formic acid. So the result obtained in this work agrees with that reported in the literature. The IR spectrum at the second mass loss step was weak and not specific. It implied that the decomposition products at this step are complex and it is not a simple decomposition step.

Acknowledgements

This work was financially supported by the National Natural Science Foundation of China (Nos. 30570015 and 20373072), Science Fund for Creative Research Group (No. 20621502 NSFC), Science Research Foundation of Chinese Ministry of Education (No. 2006-8IRT0543), and Natural Science Foundation of Hubei Province (No. 2005ABC02).

Appendix A. Supplementary data

Supplementary data associated with this article can be found, in the online version, at doi:10.1016/j.tca.2007.04.007.

References

[1] D. Klayman, Science 228 (1985) 1049–1055.
[2] Y. Li, Y.L. Wu, Curr. Med. Chem. 10 (2003) 2197–2230.
[3] M. Jung, K. Lee, H. Kim, M. Park, Curr. Med. Chem. 11 (2004) 1265–1284.
[4] Y. Li, Y.L. Wu, Med. Trop. Mars. 58 (1998) 9–12.
[5] Qinghaosu Antimalarial Coordinating Research Group, Institute of Biophysics, Acad. Sinica, Sci. Sinica 11 (1979) 1114–1128.
[6] J.N. Lisgarten, B.S. Potter, C. Bantuzeko, R.A. Palmer, J. Chem. Crystallogr. 28 (1998) 539–543.

[7] Y.K. Wu, Acc. Chem. Res. 35 (2002) 255–259.
[8] U. Eckstein-Ludwig, R.J. Webb, I. Goethem, D.A. van Goethem, J.M. East, A.G. Lee, M. Kimura, P.M. O'Neill, P.G. Bray, S.A. Ward, S. Krishna, Nature 424 (2003) 957–961.
[9] P.M. O'Neill, G.H. Posner, J. Med. Chem. 47 (2004) 2945–2964.
[10] R.K. Haynes, B. Fugmann, J. Stetter, K. Rieckmann, et al., Angew. Chem. Int. Ed. 45 (2006) 2082–2088.
[11] A.J. Lin, D.L. Klayman, J.M. Hoch, J. Org. Chem. 50 (1985) 4504–4508.
[12] X.D. Luo, H.J.C. Yeh, A. Brossi, Heterocycles 23 (1985) 881–887.
[13] K.L. Chan, K.H. Yuen, H. Takayanagi, S. Janadasa, K.K. Peh, Phytochemistry 46 (1997) 1209–1214.
[14] H. Xing, Y. Yang, B. Su, M. Huang, Q. Ren, J. Chem. Eng. Data 48 (2003) 330–332.
[15] P. Coimbra, M.R. Blanco, H.S.R.C. Silva, M.H. Gil, H.C. de Sousa, J. Chem. Eng. Data 51 (2006) 1097–1104.
[16] E.F. Westrum Jr., G.T. Furukawa, J.P. McCullough, in: J.P. McCullough, D.W. Scott (Eds.), Experimental Thermodynamics, vol. 1. Calorimetry of Non-reaction System, Butterworths, London, 1968, p. 133.
[17] Z.C. Tan, G.Y. Sun, A.X. Yin, W.B. Wang, J.C. Ye, L.X. Zhou, J. Therm. Anal. Calorim. 45 (1995) 59–67.
[18] Z.C. Tan, G.Y. Sun, Y.J. Song, L. Wang, J.R. Han, Y.S. Liu, M. Wang, D.Z. Nie, Thermochim. Acta 247 (2000) 352–353.
[19] Z.C. Tan, L.X. Sun, S.H. Meng, L. Li, F. Xu, P. Yu, B.P. Liu, J.B. Zhang, J. Chem. Thermodyn. 34 (2002) 1417–1429.
[20] D.G. Archer, J. Phys, Chem. Ref. Data 22 (1993) 1441–1453.